MORPHOLOGY OF ALPHA PHASE IN RAPIDLY SOLIDIFIED AND WROUGHT Ti-6Al-4V ALLOY DURING ISOTHERMAL ANNEALING

I. WEISS, A.G. JACKSON*, G. WELSCH**, D. EYLON*** and F.H. FROES****

Wright State University, College of Engineering and Computer Science, Materials Science and Engineering, Dayton, OH 45435-0001, U.S.A.
**Systems Research Laboratories, A Division of Arvin/Calspan, 2800 Indian Ripple Road, Dayton, OH 45440-3696, U.S.A.*
***Case Western Reserve University, Department of Materials Science and Engineering, University Circle, 10900 Euclid Avenue, Cleveland, OH 44106-1712, U.S.A.*
****University of Dayton, Graduate Materials Engineering, KL407, Dayton, OH 45469-0001, U.S.A.*
*****U.S. Air Force Wright Aeronautical Laboratories, Materials Laboratory, AFWAL/MLLS, Wright-Patterson AFB, OH 45433-6533, U.S.A.*

ABSTRACT

The morphology of isothermally annealed alpha phase in rapidly solidified (RS) and wrought Ti-6Al-4V alloy was investigated with the aim of identifying differences in the microstructures. Beta quenched wrought and RS specimens were annealed for 24 hr at subtransus temperatures of 650 to 925°C (1200 to 1700°F) followed by water quenching. TEM was used to characterize the size and morphology of the alpha phase. Following beta quenching of the wrought alloy and the as-solidified RS material, the martensite α' phase exhibited a close packed-hexagonal structure, which changed to α and β phases upon subsequent annealing. The microstructure of wrought specimens, following annealing, displayed lenticular, high aspect ratio alpha grains. In contrast, the RS samples displayed a low aspect ratio alpha grain morphology. This change in morphology is related to the length of the α' phase and the size of the beta grains present in the two types of materials.

INTRODUCTION

The mechanical properties of alpha + beta titanium alloys are greatly affected by the morphology of the alpha and beta phases. High-aspect-ratio alpha phase is produced in Ti-6Al-4V material following cooling from above the beta transus temperature, which leads to desireable fatigue crack growth propagation rates, high creep resistance, and inferior tensile and fatigue initiation properties[1-5]. The latter properties are much improved when the alpha phase exhibits an equiaxed morphology [1,6-10].

Previous work has demonstrated that hot working, and thermo-chemical processing are effective methods for modifying the lenticular alpha phase to a more equiaxed morphology [11-21]. Recently, it was demonstrated that equiaxed alpha and beta phases can be produced in rapidly solidified (RS) Ti-6Al-4V alloy [22]. The globular alpha phase observed was found to have the same morphology as that produced in worked and heat treated material.

It was the objective of the present work to study the formation of alpha phase in RS and wrought Ti-6Al-4V alloys following recrystallization annealing (RA) treatment in order to explain the structural refinement observed in RA'D RS material.

MATERIALS AND EXPERIMENTAL PROCEDURES

Mill annealed Ti-6Al-4V plate material was used as the starting stock with a chemical composition given in Table I. The beta transus temperature of this material is approximately 995°C (1825°F) [23]. Cubes (10mm on a side) were solution treated at 1035°C (1900°F) for 15 min in air, followed by water quenching. These specimens were subsequently annealed at temperatures ranging between 650°C (1200°F) and 925°C (1700°F) for 24 hr, followed by water quenching to maintain the alpha morphology which existed at the annealing temperature [Fig. 1(a).

Wrought Ti-6Al-4V bars were electron beam melted and rapidly solidified by the PDME method to produce ribbon ∿ 2mm wide and 80 μm thick, corresponding to a cooling rate between 10^5 and 10^6°K/S [22]. The RS ribbons were vacuum annealed at temperatures between 650°C (1200°F) and 925°C (1700°F) for 24 hr followed by water quenching [Fig. 1(b). The TEM investigation was performed on 100CX and 2000FX JEOL microscopes, and EDS analysis was carried out utilizing a Tracor-Northern set-up.

*α' is defined here as transformed beta phase (martensite phase) with a HCP structure and beta phase chemical composition. α is defined here as an HCP phase with a chemical composition closer to the chemical composition, as defined from the phase diagram, of equilibrium alpha phase.

RESULTS AND DISCUSSION

a. Starting Microstructures

The microstructures shown in Fig. 2 (a) and (b) resulted from the first heat treatment cycle. Both materials displayed a martensitic structure (α').* The length of the martensite plates is limited by the beta grain size as observed in the RS specimen. Short martensite plates of up to 20 μm are observed in the RS material [Fig. 2(b)]. Longer martensite plates of about 200 μm are present in the wrought material, following beta solution treatment and water quenching as shown in Fig. 2(a). Shorter martensite plates are also observed in the wrought material, as a result of the long plates intersecting each other and the formation of short martensite plates within the beta grains.

TEM observation of the (wrought and RS) microstructures revealed the presence of microtwins across the martensite plates as shown in Figs. 3(a) and 4. Selected area diffraction taken from a wide martensite plate in wrought and RS specimens indicated that the martensite phase possesses a hexagonal close-packed crystal structure [Fig. 3(b)] with chemical composition similar to that of the beta phase.

b. Microstructure of Recrystallized Annealed Material

The microstructures of wrought and RS material following annealing at 925°C (1700°F) for 2 hr and slow cooling at a rate of 50°C/hr, second heat treatment cycle shown in Fig. 1 (a) and (b) are shown in Fig. 5(a) and (b). The wrought material displays a lenticular alpha structure with alpha plates exhibiting an average thickness of about 5 μm. Two groups of alpha plates are observed; long alpha plates of up to 200 μm nucleated at the beta grain boundaries and which subsequently grew into the beta grains, and short plates of up to 30 μm, which formed either as a result of the long alpha plates intersecting each other or by nucleation within the beta grains. The RS material, on the other hand, shows an equiaxed alpha microstructure with a mean alpha phase size of about 8 μm as shown in Fig 5(b).

c. Microstructural Development During Annealing of RS Material

In an attempt to explain the difference between the lenticular microstructure of the wrought material and the equiaxed structure of the RS material produced following recrystallization anneal treatment, TEM investigation was carried out on RS specimens annealed at different temperatures and subsequently water quenched. Following annealing at 650 and 705°C (1200 and 1300°F) for 24 hr [Fig. 6(b)and (c)] remnant of microtwins which originally formed in the martensite (α') phase [Fig. 6(a)] can be observed across the lenticular alpha martensite phase. This phase exhibits an hexagonal close-packed crystal structure with chemical composition different from that of the martensite phase. However, no major changes in the phase morphology from that of the martensite are observed, as shown in Fig. 6(b) and (c). Upon annealing at 760°C (1400°F) for 24 hr a recovered dislocation substructure is observed in locations where the microtwins used to be, as shown in Fig. 6(d). This substructure further recovers as the annealing temperature increases to 815°C (1500°F) [Fig. 6(e)]. Annealing at 925°C (1700°F) for 24 hr resulted in a low aspects ratio alpha phase, as shown in Fig. 6(f).

In earlier work [17-19], it was observed that dislocation substructures are involved with the break-up of lenticular alpha phase into a more equiaxed morphology. This occurs by diffusion of beta stabilizing elements and the creation of beta phase cusps (α/β interfaces) along the substructure (α/α interface) to lower the α/α boundary energy. Selected area diffraction patterns taken along the substructure and adjacent areas in RS specimen annealed at 760°C (1400°F) [Fig. 7(a)] were found to be almost identical as shown in Fig. 7(b) to 7(f). This indicates that these substructures are low angle boundaries with low misorientation and consequently of low energy, which, in turn, will prevent formation of beta cusps along the α/α boundaries [17-19].

In addition to the formation of recovered substructure, the martensite plates transform to α phase during annealing. The alpha phase maintains the hexagonal close-packed crystal structure of the martensite phase, as well as its morphology [Fig. 6(b)] but changes chemical composition (mainly Vanadium) to accomodate the formation of the beta phase* along the interphase boundaries as shown in Fig. 8(a). Microchemical analysis performed across the beta phase and the hexagonal closed-packed alpha phase shows enrichment of Vanadium up to 10 w/o along the interphase boundaries where beta phase is present. Significantly lower Vanadium levels of about 2 w/o were detected in the alpha phase, as shown in Fig. 8(b).

The aluminum concentration on the other hand, was found to be slightly higher in the alpha phases than the nominal aluminum level, following annealing at 760°C (1400°F) for 24 hr, indicating minimum redistribution of aluminum. Phase adjustment, which is manifested by a larger

* Beta phase is defined here as a BCC phase with a chemical composition closer to that of the chemical composition, as defined from the phase diagram, of equilibrium beta phase.

volume fraction of beta grains and smaller and more equiaxed alpha grains, is also taking place during annealing above 760°C (1400°F), as demonstrated in specimens annealed at 925°C (1700°F) [Fig. 9(a)]. The hexagonal close-packed equiaxed alpha grains [Figs. 9(a) and (b)] and the beta grains obtained following annealing at 925°C (1700°F) for 24 hr in RS material, are relatively small in size being 10 μm and about 20 μm respectively as measured in Fig. 2(b). Higher aspect ratio alpha grains and beta grains as large as 200 μm or more are observed in wrought material undergoing the same annealing treatment. Upon slow cooling to room temperature, the RS material with the smaller beta grains and equiaxed primary alpha phase transform to an equiaxed alpha grain structure with a mean grain size of about 8 μm [Fig. 2(b)]. The wrought material with large beta grains and lenticular primary alpha phase transforms to a high aspect ratio alpha grain structure as shown in Fig. 2(a).

CONCLUSIONS

1. The microstructure of wrought Ti-6Al-4V alloy following beta solution treatment and water quenching consists of long martensite plates with high aspect ratio, the result of large beta grains (200 μm and above) present prior to water quenching.
2. The microstructure of RS Ti-6Al-4V alloy following rapid solidification displays short martensite plates, the result of small beta grains (around 20 μm) present prior to final cooling.
3. The martensite plates produced in wrought and RS material contain microtwins, and they possess a hexagonal close-packed crystal structure, with chemical composition similar to that of the beta phase.
4. Martensite plates in both materials transform to alpha and beta phases during isothermal annealing. The beta phase is present at interphase boundaries and is enriched in Vanadium (up to 10 w/o). The alpha phase with lower Vanadium concentration of about 2 w/o) retains the hexagonal close-packed crystal structure of the martensite plates, little redistribution of aluminum was observed.
5. RS material transforms upon slow cooling to an equiaxed alpha grain structure. Wrought specimens with large beta grains and a lenticular primary alpha grains at the annealing temperature transform during cooling to a high aspect ratio alpha grain structure.

ACKNOWLEDGEMENTS

A. G. Jackson gratefully acknowledges support of AFWAL Contract F33615-86-C-5013.

REFERENCES

1. G. R. Yoder, L. A. Cooley, and T. W. Crooker, 23rd Structures, Structural Dynamics and Materials Conference, New Orleans, LA, May 1982, pp. 132-36.
2. S. M. Sastry, P. S. Pao, and K. K. Sankaran, Titanium '80, Science and Technology Vol. 2, edited by H. Kimura O. Izumi, AIME, Warrendale, PA, 1980, pp. 873-86.
3. D. Eylon, J. A. Hall, C. M. Pierce, and D. L. Ruckle, Metall. Trans. A, Vol. 7A, 1976, pp. 1817-26.
4. F. H. Froes, J. C. Chesnutt, R. G. Berryman, G. R. Keller, and W. T. Highberger, 10th National SAMPE Technical Conference, Kiamesha, NY, 1978, pp. 511-33.
5. F. H. Froes and W. T. Highberger, Journal of Metals, vol. 32, 1980, pp. 57-64.
6. D. Eylon, M. E. Rosenblum, and S. Fujishiro, Titanium '80, Science and Technology, Vol. 2, AIME, Warrendale, PA, 1980, pp. 1845-54.
7. D. Eylon and C. M. Pierce, Metall. Trans. A, vol. 7A, 1976, pp. 111-21.
8. P. Dadras and and J. F. Thomas, Jr., Metal. Trans. A, vol. 12A, 1981, pp. 1867-76.
9. S. L. Semiatin and G. D. Lahoti, Metal. Trans. A, vol. 12A, 1981, pp. 1705-17.
10. C. C. Chen, Report RD 77-110, Research and Development, Wyman-Gordon Company, North Grafton, MA, 1977.
11. F. H. Froes, J. C. Chesnutt, R. G. Berryman, G. R. Keller, and W. T. Highberger, 10th National SAMPE Technical Conference, Kiamesha Lake, NY, (1978), p. 511.
12. M. Peters, A. Gysler, and G. Luetjering, Titanium '80, Science and Technology, vol. 2, edited by H. Kimura and O. Izumi, AIME, Warrendale, PA (1980), p. 925.
13. M. Peters and G. Luetjering, Titanium '80, Science and Technology, vol. 2, edited by H. Kimura and O. Izumi, AIME, Warrendale, PA (1980), p. 925.
14. H. Margolin and P. Cohen, in Titanium '80, Science and Technology, vol. 2, edited by H. Kimura and O. Izumi, AIME, Warrendale, PA (1980), p. 1555.
15. M. Peters, G. Luetjering, and A. Gysler, Z. Metallkunde Bd 74, p. 274
16. A. Gogia, D. Banerjee and D. C. Birla, Trans. Indian Inst. Metals, vol. 36, 1983, pp. 200-07.
17. I. Weiss, G. Welsch, F. H. Froes and D. Eylon, Titanium Science and Technology, edited by G. Lutjering, V. Zwicker and W. Bunk, Dgfm, Oberursel, FRG, 1985, pp. 1503-1510.
18. I. Weiss, G. Welsch, F. H. Froes and D. Eylon, Proc. of 7th Int'l. Conference on Strength of Metals and Alloys, Montreal, Canada, 1985, pp. 1073-1078.

19. I. Weiss, F. H. Froes, D. Eylon and G. Welsch, Metall. Trans. A., 1986, Vol. 17A, 1986, pp. 1935-47.
20. W. R. Kerr, P. R. Smith, M. E. Rosenblum, F. J. Gurney, Y. R. Mahajan, and L. R. Bidwell, Titanium '80, Science and Technology, Vol. 4, (edited by H. Kimura and O. Izumi), vol. 4, AIME, Warrendale, PA (1980), p. 2477.
21. L. Levin, R. G. Vogt, D. Eylon and F. H. Froes, edited by G. Lutjering, V. Zwicker and W. Bunk, Oberursel, FRG, 1985, pp. 2107-2114.
22. T. F. Broderick, A. G. Jackson, H. Jones and F. H. Froes, Metall. Trans. A., vol 16A, 1985, pp. 1551-1959.
23. C. F. Yolton, R. F. Malone, and F. H. Froes, Metall. Trans. A, Vol. 10A, 1979, pp. 132-34.

TABLE I
CHEMICAL COMPOSITION

	Al	V	Fe	C	N	O	H	Ti
weight pct	6.7	4.1	0.18	0.01	0.013	0.16	0.004	Balance

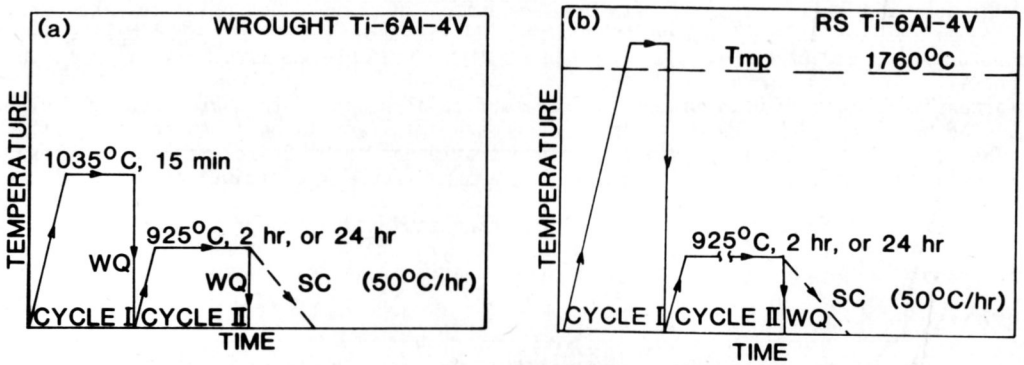

Figure 1. Heat treatment sequences applied to wrought and RS Ti-6Al-4V. The two cycles (I) represent formation of starting microstructure (II) annealing treatment.

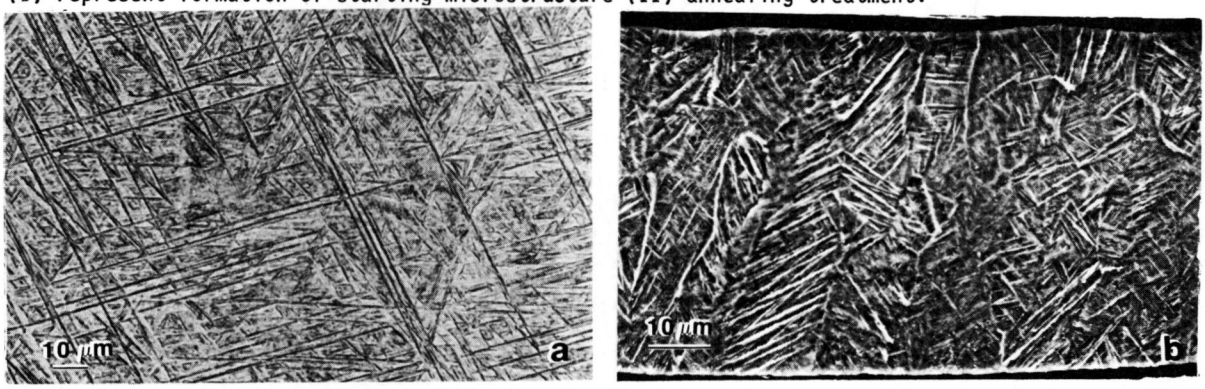

Figure 2. Starting microstructure following the first heat treatment cycle (a) wrought material annealed at 1035°C for 15 min/WQ (b) RS material in the as-solidified condition.

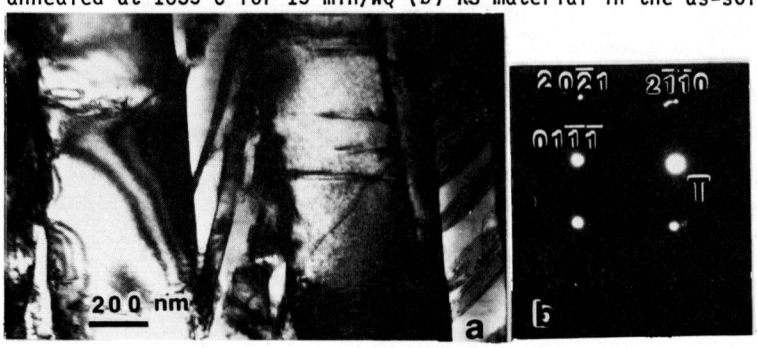

Fig 3. TEM micrograph of wrought specimen following beta solution treatment and water quenching. (a) Martensite plates containing micro-twins; (b) selected area diffraction taken from a wide martensite plate, indicating that the martensite phase possesses an HCP crystal structure. [0112]α-Ti.

Fig. 5. Microstructures of wrought and RS material following second heat treatment cycle; annealing at 925°C for 2 hr and slow cooling at 50°C/hr. (a) Wrought material with lenticular α grain structure; (b) RS specimen; with equiaxed grain structure.

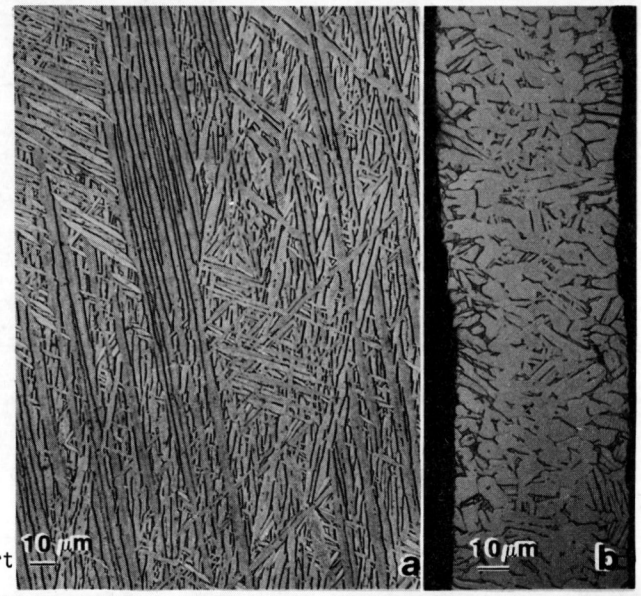

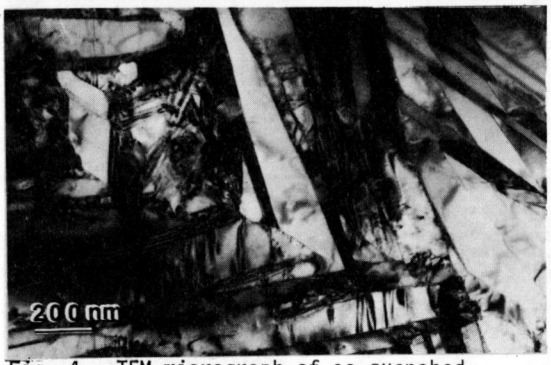

Fig. 4. TEM micrograph of as-quenched RS specimen. This microstructure displays short martensite plates with microtwins.

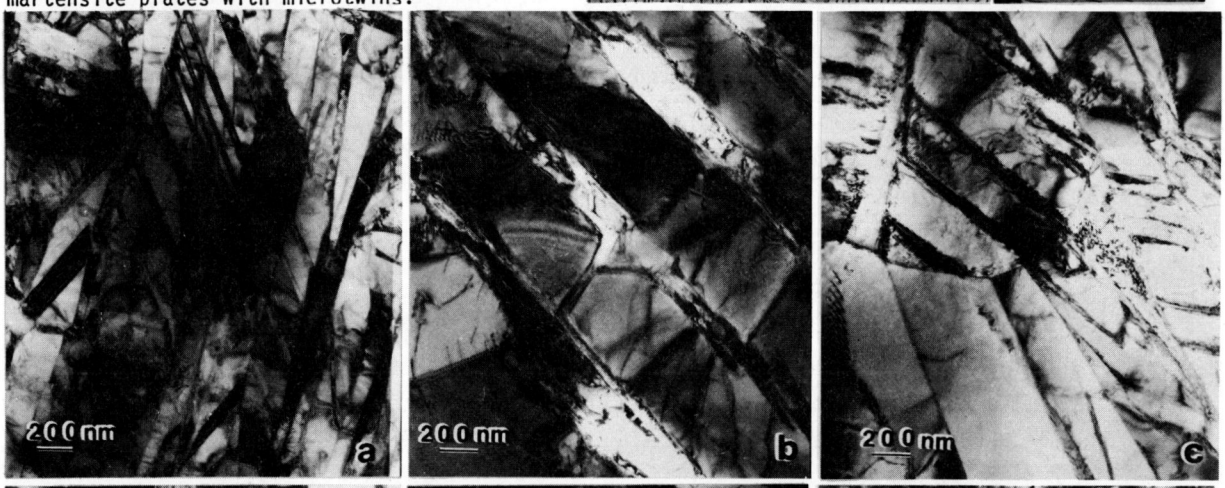

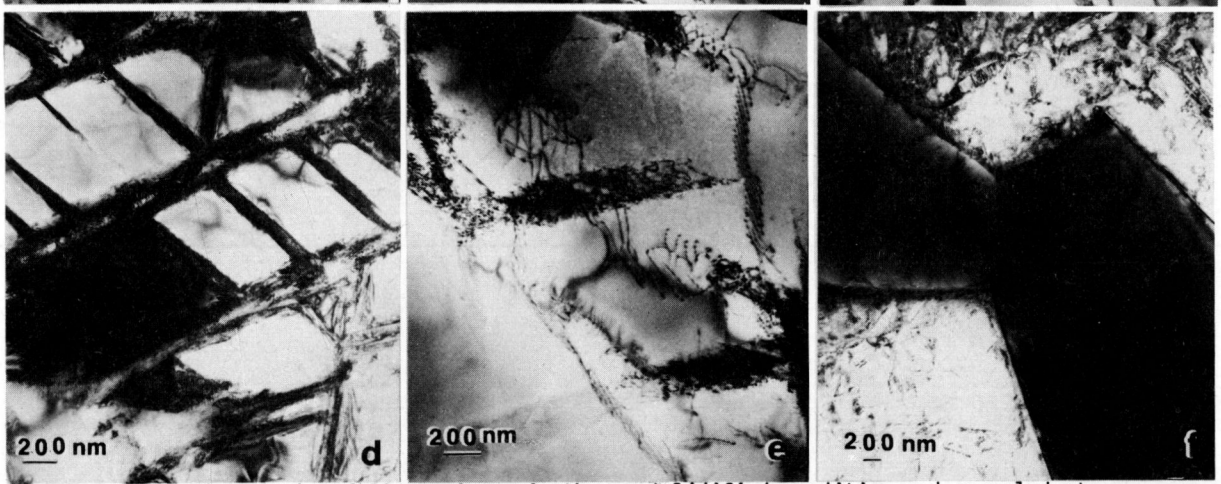

Figure 6. TEM micrographs of RS specimens in the as-solidified condition and annealed at temperatures ranging between 650°C and 925°C for 24 hr/WQ. (a) As-solidified condition; after annealing for 24 hr/WQ at (b) 650°C (c) 705°C (d) 700°C (e) 815°C (f) 925°C.

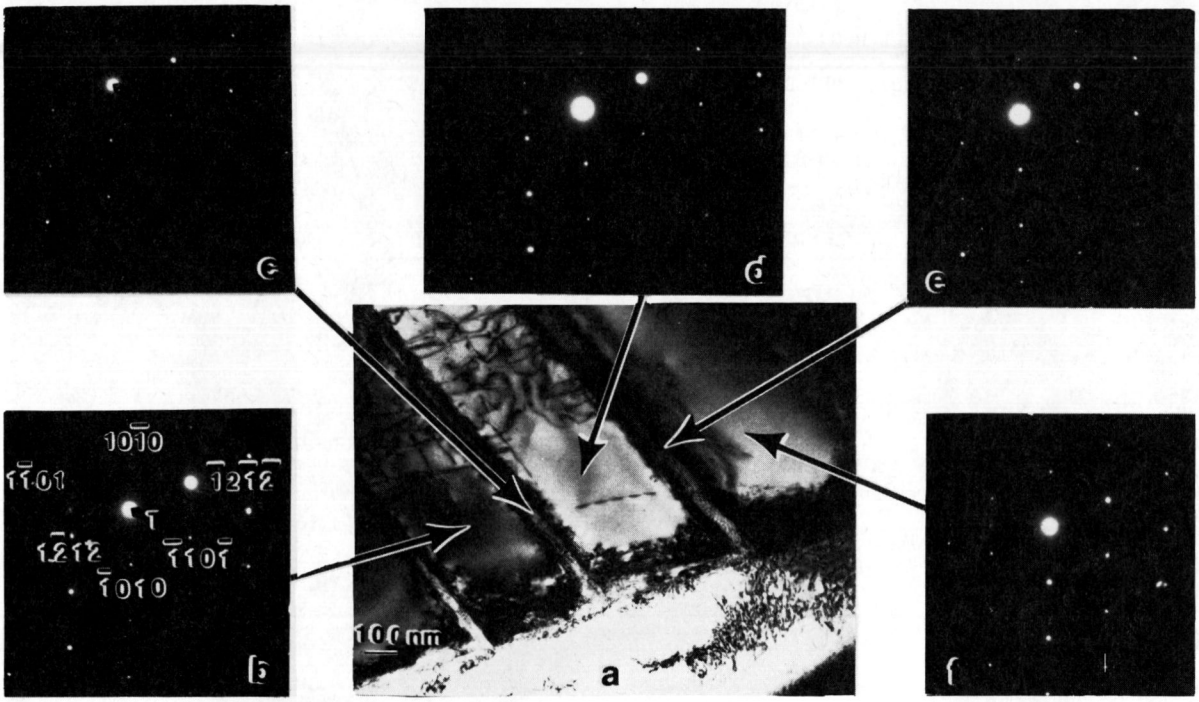

Figure 7. TEM micrograph of (a) substructure; (b) - (f) SAD patterns from areas as marked [1$\bar{2}$13] α-Ti zone.

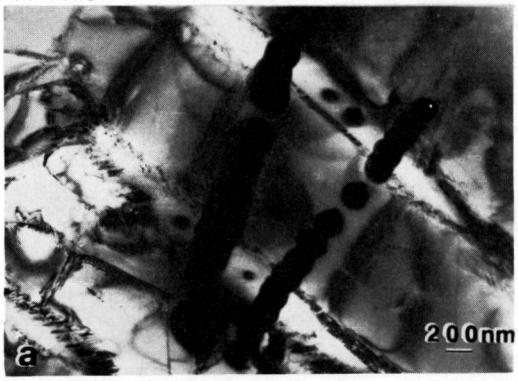

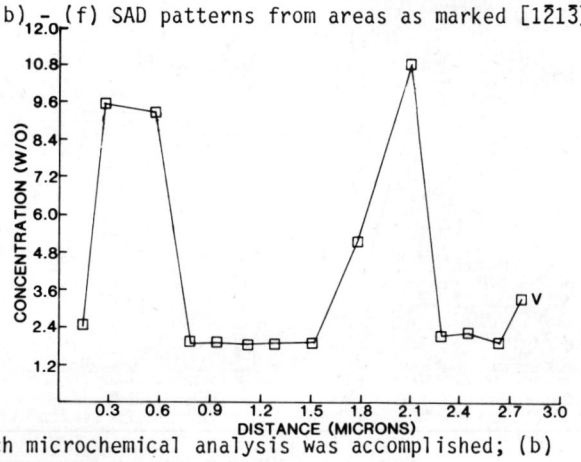

Figure 8. (a) TEM micrograph of region on which microchemical analysis was accomplished; (b) plot of concentration of V as function of position.

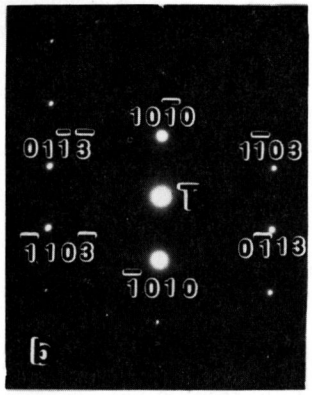

Figure 9. TEM micrograph of RS alloy showing hexagonal close-packed equiaxed grains (a) α, after annealing at 925°C/24 hr; (b) SAD of [01$\bar{1}$2] α-Ti zone in equiaxed grain.